NIH Public Access
Author Manuscript
Traffic. Author manuscript; available in PMC 2013 June 01.

Published in final edited form as:
Traffic. 2012 June ; 13(6): 857–868. doi:10.1111/j.1600-0854.2012.01351.x.

A Triple Arg Motif Mediates α_{2B}-Adrenergic Receptor Interaction with Sec24C/D and Export

Chunmin Dong[1], **Charles D. Nichols**[1], **Jianhui Guo**[2], **Wei Huang**[2], **Nevin A. Lambert**[2], and **Guangyu Wu**[1,2,*]

[1]Department of Pharmacology and Experimental Therapeutics, Louisiana State University Health Sciences Center, 1901 Perdido St, New Orleans, LA 70112.

[2]Department of Pharmacology and Toxicology, Georgia Health Sciences University, Augusta, GA 30912.

Abstract

Recent studies have demonstrated that cargo exit from the endoplasmic reticulum (ER) may be directed by ER export motifs recognized by components of the COPII vesicles. However, little is known about ER export motifs and vesicle targeting of the G protein-coupled receptor (GPCR) superfamily. Here we have demonstrated that a triple Arg (3R) motif in the third intracellular loop functions as a novel ER export signal for α_{2B}-adrenergic receptor (α_{2B}-AR). The 3R motif mediates α_{2B}-AR interaction with Sec24C/D and modulates ER exit, cell surface transport, and function of α_{2B}-AR. Furthermore, export function of the 3R motif is independent of its position within α_{2B}-AR and can be conferred to CD8 glycoprotein. These data provide the first evidence implicating that export of GPCRs is controlled by code-directed interactions with selective components of the COPII transport machinery.

Keywords

G protein-coupled receptor; adrenergic receptor; intracellular loop; endoplasmic reticulum; cell surface transport; export motif; Sec24; COPII vesicle

Introduction

G protein-coupled receptors (GPCRs) represent the largest superfamily of cell surface receptors that modulate a variety of cell functions in response to a broad spectrum of extracellular stimuli. Dysfunction of the GPCR systems is closely associated with the pathogenesis of many human diseases for which the receptors are the actual therapeutic targets (1–4). All GPCRs share a common molecular topology with a hydrophobic core of seven membrane-spanning α-helices, three intracellular loops, three extracellular loops, an N-terminus outside the cell, and a C-terminus inside the cell. The function of GPCRs is mediated largely through coupling to heterotrimeric G proteins, which in turn activate downstream effectors, such as protein kinases, adenylyl cyclases, phospholipases, and ion channels. The magnitude of a ligand-elicited cellular response is at least in part dictated by the number of the receptors expressed at the cell surface which are available for binding to ligands. The cell surface expression of GPCRs at a given time is determined by elaborately regulated trafficking processes, including export of newly synthesized receptors from the

*Corresponding author: Guangyu Wu, Department of Pharmacology and Toxicology, Georgia Health Sciences University, Augusta, GA 30912. Tel: 706-721-0999. Fax: 706-721-2347. guwu@georgiahealth.edu.

NIH-PA Author Manuscript
NIH-PA Author Manuscript
NIH-PA Author Manuscript

NIH-PA Author Manuscript

NIH-PA Author Manuscript

NIH-PA Author Manuscript

endoplasmic reticulum (ER) to the cell surface, endocytosis of the cell surface receptors to the endosomal compartment, recycling of internalized receptors from endosomes to the cell surface, and transport of receptors to lysosomes for degradation. Over the past decades, most studies on GPCR trafficking have focused on the events involved in the internalization, recycling and degradation of the receptors and these studies have greatly advanced our understanding of intracellular trafficking of GPCRs (1, 5–9). In contrast, the molecular mechanisms underlying GPCR exit from the ER and transport to the cell surface are largely unknown.

Exit of nascent cargo from the ER is mediated through COPII-coated transport vesicles that can be formed from three components: the small GTPase Sar1, the Sec23/24 heterodimer, and the Sec13/31 heterodimer (10–13). The assembly of COPII vesicles is initiated by GDP/GTP exchange on the Sar1 GTPase, which is catalyzed by the ER localized transmembrane guanine nucleotide exchange factor Sec12. The GTP-bound Sar1 then recruits the inner coats Sec23/24 complex to the ER exit sites to form a pre-budding complex, which then recruits the outer coat complex Sec13/31 to form the COPII vesicles. The hydrolysis of GTP to GDP of Sar1 GTPase triggers the coat to depolymerize and the release of the COPII vesicles from the ER membrane.

A number of recent studies have demonstrated that ER export is a selective process and the recruitment of cargo to COPII vesicles is mediated by ER export motifs. Several ER export motifs have been identified with di-acidic and di-hydrophobic motifs being well characterized. The di-acidic motifs have been found in the cytoplasmic C-termini of a number of membrane proteins, such as vesicular stomatitis viral glycoprotein (VSVG), cystic fibrosis transmembrane conductance regulator (CFTR), ion channels, and the yeast membrane proteins Sys1p and Gap1p (14–20). The DxE motif (16, 17, 20), together with neighboring residues (21) directs the concentration of the cargo molecule during export from the ER thereby enhancing the rate of its exit from the ER. Mutation of the DxE motif results in a VSVG molecule which assembles correctly but exits the ER at a slower rate. The dihydrophobic motifs are required for efficient transport of the ERGIC-53, p24 family of proteins, and the Erv41–Erv46 complex from the ER to the Golgi (22–25).

The function of ER export motifs to enhance the recruitment of the cargo on ER exit sites may be mediated through direct interaction with components of the COPII vesicles, particularly the Sec24 subunit (15, 19, 26–29). There are four Sec24 isoforms (Sec24A, Sec24B, Sec24C, and Sec24D) identified in human cells and these can be further divided into Sec24A/B and Sec24C/D subclasses based on the sequence homology. Three cargo recognition sites have been mapped in Sec24 (27, 29), demonstrating that different ER-export motifs interact with the same COPII component to facilitate ER export. Meanwhile, different ER export motifs may have selectivity towards distinct Sec24 isoforms (28).

It has been well described that the C-terminus, particularly the membrane-proximal portion, is required for ER export of a number of GPCRs, including rhodopsin, vasopressin V2, dopamine D1, adenosine A1, α_{2B}-adrenergic (α_{2B}-AR), angiotensin II type 1, melanin-concentrating hormone receptor 1 and luteinizing hormone/choriogonadotropin receptors. Several motifs essential for GPCR transport from the ER to the cell surface have also been identified in this region (30–36). Although the molecular mechanisms underlying the function of these motifs in controlling GPCR export remain elusive, several studies suggest that they are likely involved in the regulation of proper receptor folding in the ER (31, 34, 37) and none of these motifs have been shown to directly link to the COPII vesicles. Therefore whether or not linear ER export motifs exist among the GPCR superfamily and if so, whether they modulate receptor transport to the functional destination and cellular responses to a given signal are unknown.

NIH-PA Author Manuscript

NIH-PA Author Manuscript

NIH-PA Author Manuscript

To address these issues, we used α_{2B}-AR as a model to investigate GPCR interaction with Sec24 subunits. By using progressive deletion, site-directed mutagenesis and protein-protein interaction assays, we have revealed that three basic Arg residues (3R), which is highly conserved in the GPCR superfamily, in the third intracellular loop (ICL3) mediate α_{2B}-AR interaction with Sec24C/D isoforms. Mutation of the 3R motif attenuates α_{2B}-AR exit from the ER, transport to the cell surface, and activation of downstream signaling molecules. Furthermore, the 3R motif can facilitate α_{2B}-AR export trafficking when transferred to the C-terminus and also enhances CD8 glycoprotein transport to the cell surface. These data demonstrate that the 3R motif represents a novel ER export motif and provide the first evidence indicating that GPCR export from the ER is directed by a specific code which mediates receptor interaction with components of the COPII transport vesicles.

Results

The ICL3 of α_{2B}-AR selectively and directly interacts with Sec24C/D isoforms

One of the most important features for ER export motifs is to mediate cargo interaction with the Sec24 subunit of ER-derived COPII vesicles (15, 19, 26, 27). To define if the GPCR superfamily utilizes ER export motifs to exit from the ER, we used α_{2B}-AR as a representative to determine if its cytoplasmic domains could physically associate with Sec24. The first (ICL1 – 10 residues), the second (ICL2 – 15 residues), and the third (ICL3 – 165 residues) intracellular loops and the C-terminus (CT - 24 residues) of α_{2B}-AR were generated as GST fusion proteins and their interaction with different Sec24 isoforms was measured by GST fusion protein pull-down assay (Fig. 1A). The GST fusion proteins encoding the ICL3, but not the ICL1, the ICL2, and the C-terminus, bound to Sec24D (Fig. 1A). The interaction of the ICL3 with Sec24C and Sec24D isoforms was much stronger than that with Sec24A and Sec24B isoforms (Fig. 1B). These data demonstrate that the ICL3 preferentially interacts with Sec24C/D.

To determine if the interaction between the ICL3 of α_{2B}-AR and Sec24 is direct, Sec24D was purified from insect Sf9 cells using the Bac-To-Bac baculovirus expression system (Fig. 1C) and incubated with GST-ICL3 fusion proteins. The GST fusion proteins encoding the ICL3, but not the ICL1, the ICL2, and the C-terminus, interacted with purified Sec24D (Fig. 1D).

The triple Arg (3R) motif is a Sec24-binding site in α_{2B}-AR

The progressive deletion strategy was first utilized to define a subdomain in the ICL3 mediating α_{2B}-AR interaction with Sec24D. The GST fusion proteins of the ICL3 fragments R285-E369, N327-E369 and G349-E369 interacted with Sec24D, whereas the fragments K205-P284, R285-C326, N327-L348 and L339-Q358 did not (Fig. 2A and 2B). These data reveal the Sec24-binding site in the region 359WWRRRTQLSRE369 (Fig. 2A).

To precisely identify specific residues mediating the ICL3 interaction with Sec24, each of the 11 amino acid residues in the domain 359WWRRRTQLSRE369 was mutated to Ala by site-directed mutagenesis and the effect of mutation on the ICL3 interaction with Sec24D determined by GST fusion protein pull-down assay. Mutation of R361, R362 and R363 almost abolished the ICL3 interaction with Sec24D (Fig. 2C). In contrast, mutation of W359, W360, Q365, S367, R368 and E369 did not significantly influence the ICL3 interaction with Sec24D and mutation of T364 and L366 moderately enhanced the interaction (Fig. 2C). Combinational mutation of R361, R362 and R363 (3R) to three Ala (3A), three non-charged Gln (3Q), or three negatively charged Glu (3E) completely blocked the ICL3 interaction with Sec24D, whereas mutation of 3R to three positively charged Lys (3K) did not alter the ICL3 binding to Sec24D (Fig. 2D). Furthermore, increase in the

NIH-PA Author Manuscript

NIH-PA Author Manuscript

NIH-PA Author Manuscript

concentration of NaCl to 400 mM in the binding buffer markedly blocked the ICL3 interaction with Sec24D (Fig. 2E). These data suggest that the 3R motif mediates ICL3 interaction with Sec24 and the interaction between the ICL3 and Sec24 is likely ionic.

To exclude the possible interference of GST on the ICL3 interaction with Sec24, a 21 residue peptide of the ICL3 (from G349 to E369) containing the 3R motif and a mutated peptide in which the 3R motif was mutated to 3A were synthesized and conjugated to agarose. Peptide-conjugated agarose beads were then used to measure the interaction between the ICL3 and four Sec24 isoforms. Similar to the data obtained from the GST fusion protein pull-down assay, the ICL3 peptide-conjugated agarose beads, but not Agorose alone (data not shown), preferentially interacted with Sec24C and Sec24D isoforms over Sec24A and Sec24B isoforms. Mutation of the 3R motif to 3A markedly inhibited the interaction of the ICL3 with Sec24 (Fig. 3A). The ICL3 also interacted with endogenous Sec24D in a 3R motif-dependent fashion as measured in both GST fusion protein (Fig. 3B) and peptide-conjugated agarose (Fig. 3C) pull-down assays. Furthermore, mutation of the 3R motif abolished the interaction of GST-ICL3 fusion proteins with purified Sec24D (Fig. 3D).

We then determined the interaction between full-length α_{2B}-AR and Sec24D by co-immunoprecipitation. α_{2B}-AR or its 3A mutant in which the 3R motif were mutated to 3A were tagged with HA at their N-termini and transiently expressed together with GFP-tagged Sec24D in HEK293 cells. α_{2B}-AR was immunoprecipitated by anti-HA antibodies and Sec24D in the immunoprecipitate was detected by immunoblotting using anti-GFP antibodies. The amount of Sec24D found in the anti-HA immunoprecipitates from cells expressing α_{2B}-AR was much higher than that from cells expressing the 3A mutant (Fig. 3E and 3F). These data suggest that the 3R motif mediates α_{2B}-AR interaction with Sec24.

The 3R motif controls α_{2B}-AR exit from the ER

We next determined if the function of the 3R motif, via interacting with Sec24C/D, is to modulate α_{2B}-AR targeting to COPII vesicles. In the first series of experiments, we took advantage of our previously characterized Golgi-localized YS mutant of α_{2B}-AR (38) and determined if mutation of the 3R motif could block its transport from the ER to the Golgi. In both HEK293 and COS7 cells, mutation of the YS motif to Ala (YS-2A) clearly induced an accumulation of α_{2B}-AR in the Golgi as the mutated receptor was co-localized with the Golgi marker GM130 (Fig. 4A and 4C). Further mutation of the 3R motif to 3A (YS/3R-5A) strongly arrested α_{2B}-AR in the ER and the mutated receptor was strongly co-localized with the ER marker calregulin (Fig. 4A and 4D). Quantitative data showed that more than 60% of cells had Golgi-localized α_{2B}-AR in cells expressing the YS-2A mutant, whereas less than 20% of cells contained Golgi-localized α_{2B}-AR in cells expressing the YS/3R-5A mutant (Fig. 4B).

In the second series of experiments, we chose those COS7 cells in which the YS-2A or YS/3R-5A mutants were located in the Golgi to study the kinetics of α_{2B}-AR transport to the Golgi in the FRAP assay after the Golgi-localized receptors were photobleached in living cells. After photobleaching the intensities of the Golgi-localized YS-2A and YS/3R-5A mutants were markedly reduced and they were unable to recover to the prebleach intensities, suggestive of a large number of the immobilized α_{2B}-AR in the Golgi. The recovery of the YS-2A mutant after photobleaching was much faster than that of the YS/3R-5A mutant (Fig. 4E). The half-time of the recovery of the YS-2A mutant was much shorter than that of the YS/3R-5A mutant (Fig. 4F). These data demonstrate that the mutation of the 3R motif in α_{2B}-AR induces defective transport to the Golgi.

NIH-PA Author Manuscript

NIH-PA Author Manuscript

NIH-PA Author Manuscript

The 3R motif and Sec24D modulate the cell surface transport and signaling of α_{2B}-AR

To determine if α_{2B}-AR interaction with Sec24 modulates its transport to the functional destination, we first determined the effect of mutating the 3R motif on its cell surface expression at the steady state. α_{2B}-AR and its 3A mutant were transiently expressed in HEK293 cells and their expression at the cell surface was measured by ligand binding of intact live cells using the radioligand ^{3}H-RX821002. To exclude the possible influence of the mutation on the ligand binding ability of α_{2B}-AR, the cell surface expression of α_{2B}-AR and its 3A mutant was also measured by flow cytometry following staining with anti-HA antibodies in nonpermeabilized cells. The cell surface expression of the 3A mutant was moderately but significantly lower by approximately 25% than that of α_{2B}-AR (Fig. 5A). In contrast, mutation of W360, a 3R motif neighboring residue, did not influence the cell surface expression of α_{2B}-AR and the total expression was comparable between α_{2B}-AR and its 3A mutant as determined by measuring the total fluorescence in cells expressing GFP-tagged receptors (Fig. 5A). Furthermore, α_{2B}-AR and its 3A mutant similarly underwent internalization in response to epinephrine stimulation. After epinephrine stimulation for 10, 20 and 30 min, the cell surface expression of α_{2B}-AR was reduced by 26 ± 3, 35 ± 4 and 30 ± 3%, respectively. Under the same time points, the cell surface expression of the mutant 3A was attenuated by 27 ± 3, 35 ± 5 and 31 ± 4%, respectively. These data suggest that the 3R motif may not play a major role in internalization of α_{2B}-AR.

We then sought to investigate if the reduction in the cell surface expression of α_{2B}-AR induced by mutating the 3R motif could ultimately alter signal transduction of the receptor. ERK1/2 activation by UK14304, an α_2-AR agonist, was clearly attenuated in cells expressing the 3A mutant as compared with cells expressing wild-type α_{2B}-AR (Fig. 5B and 5C).

We next chose Sec24B and Sec24D as representatives to determine the effect of shRNA-mediated knockdown on the cell surface expression of α_{2B}-AR in HEK293 cells. Consistent with previous reports (39), transient expression of Sec24B and Sec24D shRNA knocked down endogenous Sec24B and Sec24D, respectively, by about 85%. Similar to the effect of mutating the 3R motif, expression of Sec24D shRNA reduced the cell surface expression of α_{2B}-AR by about 30% (Fig. 6A), whereas knockdown of Sec24B did not alter the cell surface expression of α_{2B}-AR, consistent with selective interaction of Sec24 isoforms with the ICL3 of α_{2B}-AR. ERK1/2 activation was also similarly reduced in cells expressing Sec24D shRNA as compared with cells expressing control shRNA vector (Fig. 6B and 6C). These data suggest that different Sec24 isoforms are differentially involved in the regulation of α_{2B}-AR transport to the cell surface.

The 3R motif modulates α_{2B}-AR transport when grafted to the C-terminus

As ER export motifs identified so far are exclusively located in the cytoplasmic C-terminal portions of cargo proteins, we next asked if the export function of the 3R motif in α_{2B}-AR depends on its precise localization in the ICL3. We first determined if addition of an extra 3R motif at the C-terminus of wild-type α_{2B}-AR (WT3R) could influence its cell surface expression (Fig. 7A). Conjugation of an additional 3R motif to the C-terminus significantly promoted the cell surface transport of α_{2B}-AR by approximately 30% (Fig. 7B). Mutation of the C-terminal 3R motif to 3A (WT3A) completely reversed this effect and the cell surface expression of WT3A was similar to that of wild-type α_{2B}-AR (Fig. 7B).

We then determined if adding the 3R motif to the C-terminus could rescue the cell surface expression of the 3A mutant in which the 3R motif in the ICL3 was mutated (Fig. 7A). As compared with wild-type α_{2B}-AR, the cell surface expression of the 3A mutant was significantly lower by 30%. Addition of the 3R motif onto the C-terminus of the 3A mutant

NIH-PA Author Manuscript

NIH-PA Author Manuscript

NIH-PA Author Manuscript

almost completely restored its cell surface transport to the level similar to wild-type α_{2B}-AR, and this rescue effect was abolished by mutating the 3R motif to 3A (Fig. 7B). These data suggest that the 3R motif can facilitate α_{2B}-AR cell surface transport either in the ICL3 or in the C-terminus.

To further confirm the effects of the C-terminal 3R motif on the cell surface expression of α_{2B}-AR, we measured ERK1/2 activation in response to UK14034 stimulation in cells expressing α_{2B}-AR and its various mutants. The magnitudes of ERK1/2 activation by α_{2B}-AR and its mutants are mostly parallel with the cell surface expression of these receptors (Fig. 7C and 7D).

The 3R motif confers its export ability to CD8 glycoprotein

We then wondered if the export function of the 3R motif in α_{2B}-AR is transferable to other proteins. For this purpose, we generated chimeras in which the extracellular domain of CD8 glycoprotein was conjugated to the N-terminus of the 7th transmembrane domain (TM7) and the C-terminus of α_{2B}-AR, whereas a fragment of the ICL3 that contains either 3R (CD8-3R) or 3A (CD8-3A) was linked to the C-terminus (Fig. 8A). The cell surface expression of the chimera CD8-3A was markedly lower than that of the chimera CD8-3R as measured by flow cytometry following staining with anti-CD8 antibodies in nonpermeabilized cells (Fig. 8B). In contrast, there was no clear difference in the total expression between two chimeric proteins (Fig. 8B). Consistently, immunostaining studies revealed cell surface expression of the chimeric protein CD8-3R, whereas CD8-3A was almost undetectable at the cell surface (Fig. 8C). These data demonstrate that the 3R motif in α_{2B}-AR is sufficient to direct the export of CD8 glycoprotein to the cell surface.

Discussion

The 3R motif represents the first motif in the GPCR superfamily which mediates receptor interaction with the COPII transport machinery

The recruitment of membrane proteins into the COPII-coated vesicles is mediated by ER export motifs located in the cytoplasmic portions of cargo proteins, which are able to bind to components of COPII vesicles, primarily Sec24 subunits (27, 29, 40). Several ER export motifs have been identified in non-GPCR membrane proteins, including DxE, FF, R/KxR/K, LxxLE, and IxM motifs. However, the molecular mechanism underlying the export of nascent GPCRs from the ER and recruitment of the receptors onto the COPII vesicles are poorly defined. As an initial approach to address these issues, we investigated the interaction between Sec24 isoforms and the cytoplasmic domains of α_{2B}-AR. We found that the ICL3, but not other intracellular domains, specifically interacted with Sec24. First, the ICL3 generated as GST fusion proteins or conjugated with agarose beads bound both exogenously expressed and endogenous Sec24; second, the ICL3 bound to purified Sec24D, suggestive of a direct interaction; third, Sec24 and full-length α_{2B}-AR can form a complex as measured by co-immunoprecipitation, suggesting that the interaction may occur in native cellular environment; fourth, more interestingly, mutation of the 3R motif to Ala, Gln and Glu markedly attenuated or abolished interaction of the ICL3 or full-length α_{2B}-AR with Sec24, whereas mutation of the 3R motif to 3K preserved the interaction, suggesting that ionic interaction likely play an important role in mediating α_{2B}-AR-Sec24 interaction. Therefore, the 3R motif represents the first motif in the GPCR superfamily which is able to interact with Sec24. These data provide the first evidence indicating that GPCRs may physically associate with components of the COPII vesicles.

It has been described that different ER export motifs may preferentially interact with certain Sec24 isoforms. For example, whereas the FF motif may bind to all four Sec24 isoforms, the

NIH-PA Author Manuscript

NIH-PA Author Manuscript

NIH-PA Author Manuscript

IxM motif selectively binds to Sec24C/D and the LxxLE and DxE signals specifically bind to Sec24A/B (28). Different di-hydrophobic motifs bind Sec24 isoforms with differential affinity (41). Here we have demonstrated that α_{2B}-AR interaction with Sec24C/D was much stronger than that with Sec24A/B and mutation of the 3R motif almost abolished the interaction. These data indicate that the 3R motif specifically mediates α_{2B}-AR interaction with Sec24C/D. These data further support the notion that the ER sorting signals may have selectivity towards distinct Sec24 isoforms (28).

The 3R motif functions as a novel ER export code to direct α_{2B}-AR exit from the ER

The ER export motif-mediated interaction between cargo molecules and Sec24 enhances concentration of the cargo on ER exit sites and facilitates cargo export from the ER (15–17, 19, 26, 27). To determine the function of the 3R motif in modulating α_{2B}-AR exit from the ER, we compared the effect of mutating the 3R motif to disrupt the Sec24 interaction on the subcellular localization of α_{2B}-AR and a previously characterized Golgi-localized YS mutant (38). The α_{2B}-AR 3A mutant lacking the Sec24-binding site was accumulated in the ER and less able to transport to ER exit sites. Furthermore, mutation of the 3R motif reduced the rate of the YS mutant to transport from the ER to the Golgi. These data are consistent with the function of Sec24 interaction with ER export motifs and demonstrate that the 3R motif is required for α_{2B}-AR recruitment onto ER exit sites on the ER membrane and subsequent export from the ER. Therefore, we conclude that the 3R motif functions as a novel ER export motif interacting with Sec24C/D isoforms and promoting α_{2B}-AR export from the ER. More importantly, triple basic residues are highly conserved in the ICL3 of GPCRs (Fig. 9). In addition, multiple basic residues are also found in the membrane-proximal regions of many other membrane proteins, such as VSVG. Therefore, they may provide a common mechanism for ER export of GPCRs as well as other membrane proteins.

It is interesting to note that dibasic motifs, including the KKxx motif and the RxR motif, have been demonstrated to function as ER retention or retrieval signals for ER resident proteins, which is likely mediated through interacting with members of the COPI coat (42). The RxR motif has also been found in γ-aminobutyric acid type B receptor ($GABA_B$), a GPCR, and is responsible for ER retention of $GABA_{B1}$ subunit without co-expression of $GABA_{B2}$ subunit (37). In addition, the dibasic R/KxR/K motifs at the C-termini of Golgi resident glycosyltransferases interact with Sar1 GTPase and promote ER exit (43). Here, we have demonstrated that the triple Arg residues located in the ICL3 may function as an ER export motif which is mediated through interacting with Sec24 subunit of the COPII coat. These data suggest that basic residues may have multiple functions in protein trafficking.

The function of the 3R motif is independent of its position and can be conferred to other proteins

The Sec24-interacting ER export motifs identified thus far are exclusively localized in the C-terminal regions of membrane proteins. In contrast, the 3R motif is localized in the ICL3 of α_{2B}-AR. The ICL3 of GPCRs have been well demonstrated to be able to interact with many proteins, including arrestins, G proteins and G protein-receptor kinases, and is involved in the regulation of intracellular trafficking and signaling of the receptors (5, 8, 9, 44–46). Because the location difference between the 3R motif and other ER export motifs, we determined whether the function of the 3R motif is dependent on its unique localization in the ICL3 of α_{2B}-AR. Surprisingly, we found that the addition of the 3R motif in the ICL3 to the C-terminus promoted the cell surface export of wild type α_{2B}-AR and completely rescued the defective cell surface transport of the 3A mutant in which the 3R motif in the ICL3 was mutated. These data strongly indicate that the export function of the 3R motif is independent of its position within α_{2B}-AR and it can work either in the ICL3 or in the C-terminus to enhance receptor export.

NIH-PA Author Manuscript

NIH-PA Author Manuscript

NIH-PA Author Manuscript

Another important property of the linear ER export motifs is that their export function can be transferred to other proteins (16, 18, 19) as long as they are accessible to the COPII transport machinery. Indeed, the export function of the diacidic motifs can be conferred to CD8 glycoprotein and $GABA_{B1}$ subunit. We have demonstrated that the export properties of the 3R motif are also transferable. In particular, transplantation of an ICL3 fragment containing the 3R motif was able to move CD8 glycoprotein to the cell surface and mutation of the 3R motif to 3A abolished this function. These data further support that the 3R motif is a novel independent ER export signal.

Significance of the 3R motif-mediated α_{2B}-AR export

ER export motifs which control ER exit of cargo proteins may or may not influence cargo cell surface expression at the steady state. Modulation of α_{2B}-AR cell surface expression at steady state by the 3R motif is particularly important, as the function of α_{2B}-AR is largely determined by the amount of the receptor expressed at the cell surface, which are available for binding to its ligands. α_{2B}-AR couples to heterotrimeric Gi proteins to regulate a variety of cellular functions and is linked to the development of many human diseases. We have demonstrated that mutation of the 3R motif to disrupt α_{2B}-AR interaction with Sec24 moderately but consistently reduced α_{2B}-AR transport to the cell surface. Consistently, shRNA-mediated knockdown of endogenous Sec24D attenuated receptor export to the cell surface. In parallel with the reduction in the cell surface expression, signal propagation of α_{2B}-AR, specifically the activation of ERK1/2 in response to UK14304 stimulation, was clearly attenuated in cells expressing the 3A mutant and Sec24D shRNA. These data demonstrate that the 3R motif not only modulates the exit of α_{2B}-AR from the ER but also influences receptor transport to the functional destination and cellular response to a given extracellular stimulus.

The efficient trafficking of GPCRs and the precise positioning of specific receptors at the cell membrane are critical aspects of integrated responses of the cell to hormones and importantly, defective GPCR transport from the ER to the cell surface is associated with the pathogenesis of a variety of human diseases, such as retinitis pigmentosa, nephrogenic diabetes insipidus and male pseudohermaphroditism. As the largest superfamily of the cell surface receptors, GPCRs are actually the major therapeutic targets. Therefore, further elucidation of the molecular mechanisms underlying the export traffic of GPCRs may provide a foundation for development of therapeutic strategies by designing specific drugs to control GPCR biosynthesis and eventually receptor function.

Materials and Methods

Plasmid constructions

α_{2B}-AR tagged with GFP at its C-terminus and tagged with three HA at its N-terminus was generated as described previously (36, 47). The GFP and HA epitopes have been used to label GPCRs resulting in receptors with similar characteristics to the wild-type receptors (38, 47–49). Arrestin-3 cDNA was provided by Dr. Jeffrey L. Benovic (Thomas Jefferson University). Human Sec24A, Sec2B, Sec24C and Sec24D cDNAs, Sec24B- and Sec24D-specific shRNA in the psiSTRIKE hMGFP, and antibodies against Sec24B and Sec24D (39) were generously provided by Dr. Randy Schekman (University of California, Berkeley, CA). Sec24 isoforms tagged with GFP were generated using the pEGFP-C3 vector and XhoI/KpnI restriction sites. The α_{2B}-AR mutant containing the ICL3 fragment WWRRRTQ in the C-terminus (WT3R) was generated using the pEGFP-N1 vector and HindIII/SalI restriction sites. To generate the α_{2B}-AR and CD8 chimeras (CD8-WT), the extracellular domains of human CD8α glycoprotein was generated by PCR using primers (forward primer, 5’-GTCACTCGAGACCATGGCCTTACCAGTGACCGCC-3’ and reverse primer

NIH-PA Author Manuscript

NIH-PA Author Manuscript

NIH-PA Author Manuscript

5’-GTTAGAATTCCCCCGCCGCTGGCCGGCAC-3’) and the α_{2B}-AR fragment containing the 7th TM, the C-terminus (from residues 404 to 453) and the ICL3 peptide WWWRRRTQ generated by using primers (forward primer, 5’-GTCAGAATTCTGCAAGGTACCGCATGGC-3’ and reverse primer, 5’-GTAC AAGCTT TCA CTG TGT CCG TCT GCG CC-3’). The two PCR products were digested with XhoI/EcoRI and EcoRI/HindIII, respectively, and then ligated into the pcDNA3.1(−) vector. The α_{2B}-AR gene segments encoding different intracellular domains or different lengths of the ICL3 were cloned into the BamH1/XhoI restriction sites of pGEX-4T-1 as described previously (50). α_{2B}-AR mutants were generated using the QuikChange site-directed deletion mutagenesis kit (Stratagene, La Jolla, CA). The sequence of each construct used in this study was verified by restriction mapping and nucleotide sequence analysis.

Cell culture and transient transfection

HEK293 and COS7 cells were cultured in Dulbecco's Modified Eagle's medium (DMEM) with 10% fetal bovine serum, 100 units/ml penicillin, and 100 μg/ml streptomycin. Transient transfection of the HEK293 cells was carried out using Lipofectamine 2000 reagent (Invitrogen) as described previously (50). The transfection efficiency was estimated to be greater than 70% based on the GFP fluorescence.

Protein-protein interaction assays

Glutathione S-transferase (GST) fusion protein interaction assay was carried out as described previously (8, 50). GST fusion proteins were expressed in bacteria and purified using a glutathione affinity matrix. GST fusion proteins immobilized on the glutathione resin were either used immediately or stored at 4 °C for no longer than 3 days. Each batch of fusion protein used in experiments was first analyzed by Coomassie Brilliant Blue staining following SDS-PAGE. For Sec24 binding to immobilized ICL3 peptides, the α_{2B}-AR ICL3 peptide NH2-GKNVGVASGQWWRRRTQLSRE-COOH and its mutant NH2-GKNVGVASGQWWAAATQLSRE-COOH were synthesized, purified by HPLC to >75% and directly conjugated to agarose beads by Biosynthesis Inc. (Lewisville, TX). GST fusion proteins (about 5 μg) tethered to the glutathione resin or the peptide-conjugated agarose beads (10 μl, approximately 13 μmol peptide) were incubated with 1 mg cell lysate prepared from HEK293 cells, 300 μg from HEK293 cells transfected with GFP-tagged Sec24, or 1 μg purified Sec24D in 300 μl of binding buffer (20 mM Tris-HCl, pH 7.4, 2% NP-40, 120 mM NaCl) at 4 °C overnight. The resin was washed 4 × 1 ml binding buffer, and the retained proteins were solubilized in 1 × SDS gel loading buffer and separated by SDS-PAGE. Bound proteins were detected by immunoblotting using anti-GFP or anti-Sec24D antibodies.

To measure α_{2B}-AR and Sec24D interaction by co-immunoprecipitation, HEK293 cells cultured on 100-mm dishes were cotransfected with 2 μg of HA-tagged α_{2B}-AR and GFP-tagged Sec24D for 36 h. The cells were harvested and lysed with 500 μl of lysis buffer containing 50 mM Tris-HCl, pH 7.4, 150 mM NaCl, 1% NP-40, 0.5% sodium deoxycholate, 0.1% SDS and Complete Mini protease inhibitor cocktail. After gentle rotation for 1 h, samples were centrifuged for 15 min at 14,000 × g and the supernatant was incubated with 50 μl of protein G Sepharose for 1 h at 4 °C to remove non-specific bound proteins. Samples were then incubated with 1 μg of anti-HA antibodies overnight at 4 °C with gentle rotation followed by incubation with 50 μl of protein G Sepharose 4B beads for 5 h. Resin was collected and washed for 3 × 5 00 μl lysis buffer without SDS. Immunoprecipitated receptors were eluted with SDS gel loading buffer, separated by 10% SDS-PAGE and visualized by immunoblotting using anti-HA antibodies. Sec24D in the immunoprecipitates was detected by using anti-GFP antibodies.

NIH-PA Author Manuscript

NIH-PA Author Manuscript

NIH-PA Author Manuscript

Purification of Sec24D from insect Sf9 cells

Sec24D was purified from insect Sf9 cells as essentially described (39) using the Bac-To-Bac baculovirus expression system (Invitrogen). Briefly, Sec24D was amplified by PCR and subcloned into XhoI and KpnI restriction sites of the pFastBac HTb vector (Invitrogen), which was then transfected into the parent bacmid in DH10Bac E. coli to form an expression bacmid. The recombinant bacmid was used to transfect insect Sf9 cells using Lipofectamine for production of recombinant baculovirus particle. Sec24D was purified by affinity chromatography using Ni-NTA Agarose under native condition (Qiagen) according to the manufacturer's protocols. The 6His tag was released from purified Sec24D by cleavage using the recombinant 6His-tagged tobacco etch virus (TEV) protease at a final concentration of 0.1μg/μl at 4 °C overnight. The 6His tag and 6His-tagged TEV were removed by Ni-NTA Agarose affinity chromatography.

Fluorescence microscopy

For fluorescence microscopic analysis of the localization of α_{2B}-AR, HEK293 and COS7 cells were grown on coverslips pre-coated with poly-L-lysine in 6-well plates and transfected with 200 ng of GFP-tagged receptors for 24 h. The cells were fixed with 4% paraformaldehyde-4% sucrose mixtures in PBS for 15 min. For fluorescence microscopic analysis of the cell surface distribution of the CD8 chimeric protein, HEK293 cells were transfected with 500 ng of CD8-3R or CD8-3A constructs for 24 h. After fixation, the cells were incubated with 5% normal donkey serum for 1 h and then with FITC-conjugated anti-CD8 antibodies for 2 h. The fluorescence was detected with a Leica DMRA2 epifluorescent microscope and images were deconvolved using SlideBook software and the nearest neighbor deconvolution algorithm (intelligent Imaging Innovations, Denver, CO) as described previously (36).

For co-localization of α_{2B}-AR with the ER marker calregulin and the Golgi marker GM130, HEK293 cells were transfected with GFP-tagged α_{2B}-AR. The cells were then permeabilized with PBS containing 0.2% Triton X-100 for 5 min, and blocked with 5% normal donkey serum for 1 h. The cells were incubated with antibodies against GM130 or calregulin at a dilution of 1:50 for 1 h. After washing with PBS (3 × 5 min), the cells were incubated with Alexa Fluor 594-labeled secondary antibody (1:1000 dilution) for 1 h at room temperature. The fluorescence was detected with a Zeiss LSM 510 Confocal Microscope.

To quantify the number of cells with α_{2B}-AR expression at the Golgi, HEK293 or COS7 cells were transfected with the GFP-tagged α_{2B}-AR mutant YS-2A or YS/3R-5A and then stained with anti-GM130 antibodies as described above. In each experiment, cell images from at least 20 randomly chosen fields of about 100 transfected cells which were indicated by the GFP signal were taken using a Leica DMRA2 microscope as described above. The cells that had clear co-localization of GFP-tagged receptor and GM130 were counted as having the receptor at the Golgi.

For fluorescence recovery after photobleaching (FRAP) experiments, COS7 cells were cultured on 29 mm glass bottom culture dishes (In Vitro Scientific, Sunnyvale, CA) and transfected with GFP-tagged α_{2B}-AR mutants. Prior to imaging, standard media was replaced with CO_2 independent media. FRAP experiments were performed on a Leica SP2-TCS confocal microscope using a 63× water immersion objective and the FRAP Wizard application. During imaging, culture dishes were maintained at 37°C using a Harvard Apparatus (Holliston, MA) temperature controller and PDMI-2 Micro Incubator. Scan settings were 256 × 256 pixel resolution at 1400 Hz. For FRAP, 20 prebleach frames were acquired (0.287 second acquisition time/frame), followed by 20 bleach frames (0.287

NIH-PA Author Manuscript

NIH-PA Author Manuscript

NIH-PA Author Manuscript

seconds/frame) with the 488 laser, followed by 200 postbleach frames acquired at 5.0 second intervals. The region of interest for bleach/recovery measurement was manually drawn around the Golgi of each cell, and the mean pixel value determined for the region of interest at each recovery time point. Data points were analyzed using Graphpad Prism 4.

Intact cell ligand binding

The cell surface expression of α_{2B}-AR in HEK293 cells was measured by ligand binding of intact live cells using [^{3}H]-RX821002 as described previously (36, 50). Briefly, HEK293 cells cultured on 6-well dishes were transiently transfected with 0.5 μg of the α_{2B}-AR plasmid and split into 12-well dishes at a density of 4×10^5 cells/well. The cells were then incubated with [^{3}H]-RX821002 (Invitrogen, 41 Ci/mmol) at a concentration of 20 nM in a total of 400 μl for 90 min. The non-specific binding was determined in the presence of rauwalscine (10 μM). After washing, the cell surface-bound ligands were extracted by 1M NaOH treatment for 2 h and counted by liquid scintillation spectrometry.

For measurement of α_{2B}-AR internalization, HEK293 cells were cultured 6-well dishes and transfected with 0.5 μg α_{2B}-AR or its 3A mutant plus 1 μg arrestin-3 for 24 h. Expression of arrestin-3 has been well demonstrated to enhance internalization of α_{2B}-AR (45, 51). After starvation for 3 h, the cells were stimulated with epinephrine at a concentration of 100 μM for 10, 20 and 30 min. The cells were washed three times with cold PBS and α_{2B}-AR expression at the cell surface was measured by intact cell ligand binding as described above.

shRNA-mediated Knockdown of Endogenous Sec24

HEK293 cells were cultured on 6-well dishes and transfected with 1 μg of control or Sec24 shRNA as described (39). Sec24 expression was determined by immunoblotting using anti-Sec24 antibodies.

Flow cytometric analysis of receptor expression (FACS)

Measurement of α_{2B}-AR cell surface expression by flow cytometry was carried pout as described previously (36). Briefly, HEK293 cells transfected with HA-tagged α_{2B}-AR were suspended in PBS containing 1% FCS at a density of 4×10^6 cells/ml and incubated with high affinity anti-HA-fluorescein (3F10) at a final concentration of 2 μg/ml at 4 °C for 30 min. After washing for 2 × 0.5 ml PBS/1% FCS, the cells were re-suspended and the fluorescence was analyzed on a flow cytometer (Dickinson FACSCalibur). To measure cell surface expression of α_{2B}-AR-CD8, HEK293 cells transfected with α_{2B}-AR-CD8 chimeric proteins were incubated with FITC-conjugated human CD8 antibodies (eBioscience, San Diego, CA) at 4 °C for 30 min. Because the staining with the anti-HA or CD8 antibodies was carried out in the non-permeabilized cells and only those proteins expressed at the cell surface were accessible to the antibodies, the measured fluorescence reflected the amount of protein expressed at the cell surface. For measurement of total α_{2B}-AR expression, HEK293 cells transfected with GFP tagged α_{2B}-AR were collected and re-suspended in PBS containing 1% FBS at a density of 8×10^6 cells/ml. The overall receptor expression was determined by measuring total GFP fluorescence on a flow cytometer as described previously (36). To measure the total expression level of α_{2B}-AR-CD8, the cells were permeabilized with 0.2% Triton X-100 in PBS for 5 min on ice before staining with anti-CD8 antibodies.

Measurement of ERK1/2 activation

HEK293 cells were cultured on 6-well plates, transiently transfected and stimulated with UK14,304 at a concentration of 1 μM for 5 min at 37 °C. ERK1/2 activation was measured as described previously (47).

NIH-PA Author Manuscript

NIH-PA Author Manuscript

NIH-PA Author Manuscript

Statistical analysis

Differences were evaluated using Student's *t* test, and $P < 0.05$ was considered as statistically significant. Data are expressed as the mean ± S.E.

Acknowledgments

This work was supported by the National Institutes of Health grants R01GM076167 (to G. Wu), R01MH083689 (to C.D. Nichols), R01GM096762 and R01GM078319 (to N.A. Lambert). We are grateful to Dr. Randy Schekman, Dr. William E. Balch, Dr. Stephen M. Lanier and Dr. Jeffrey L. Benovic for helpful discussions and sharing reagents. We also appreciate the initial efforts of Dr. Matthew T. Duvernay in the early stages of this project and superb technical assistance of Dr. Yeping Tan.

The abbreviations used are

GPCR	G protein-coupled receptor
AR	adrenergic receptor
ER	endoplasmic reticulum
GFP	green fluorescent protein
ERK1/2	extracellular signal-regulated kinase 1 and 2
PBS	phosphate-buffered saline
DMEM	Dulbecco’s modified Eagle’s medium
GST	glutathione S-transferase

References

1. Hanyaloglu AC, von Zastrow M. Regulation of GPCRs by endocytic membrane trafficking and its potential implications. Annu Rev Pharmacol Toxicol. 2008; 48:537–568. [PubMed: 18184106]
2. Rosenbaum DM, Rasmussen SG, Kobilka BK. The structure and function of G-protein-coupled receptors. Nature. 2009; 459(7245):356–363. [PubMed: 19458711]
3. Pierce KL, Premont RT, Lefkowitz RJ. Seven-transmembrane receptors. Nat Rev Mol Cell Biol. 2002; 3(9):639–650. [PubMed: 12209124]
4. Wess J. Molecular basis of receptor/G-protein-coupling selectivity. Pharmacol Ther. 1998; 80(3): 231–264. [PubMed: 9888696]
5. Wu G, Bogatkevich GS, Mukhin YV, Benovic JL, Hildebrandt JD, Lanier SM. Identification of Gbetagamma binding sites in the third intracellular loop of the M(3)-muscarinic receptor and their role in receptor regulation. J Biol Chem. 2000; 275(12):9026–9034. [PubMed: 10722752]
6. Moore CA, Milano SK, Benovic JL. Regulation of receptor trafficking by GRKs and arrestins. Annu Rev Physiol. 2007; 69:451–482. [PubMed: 17037978]
7. Tan CM, Brady AE, Nickols HH, Wang Q, Limbird LE. Membrane trafficking of G protein-coupled receptors. Annu Rev Pharmacol Toxicol. 2004; 44:559–609. [PubMed: 14744258]
8. Wu G, Benovic JL, Hildebrandt JD, Lanier SM. Receptor docking sites for G-protein betagamma subunits. Implications for signal regulation. J Biol Chem. 1998; 273(13):7197–7200. [PubMed: 9516410]
9. Wu G, Krupnick JG, Benovic JL, Lanier SM. Interaction of arrestins with intracellular domains of muscarinic and alpha2-adrenergic receptors. J Biol Chem. 1997; 272(28):17836–17842. [PubMed: 9211939]
10. Barlowe C, Orci L, Yeung T, Hosobuchi M, Hamamoto S, Salama N, Rexach MF, Ravazzola M, Amherdt M, Schekman R. COPII: a membrane coat formed by Sec proteins that drive vesicle budding from the endoplasmic reticulum. Cell. 1994; 77(6):895–907. [PubMed: 8004676]
11. Bickford LC, Mossessova E, Goldberg J. A structural view of the COPII vesicle coat. Curr Opin Struct Biol. 2004; 14(2):147–153. [PubMed: 15093828]

NIH-PA Author Manuscript

NIH-PA Author Manuscript

NIH-PA Author Manuscript

12. Gurkan C, Stagg SM, Lapointe P, Balch WE. The COPII cage: unifying principles of vesicle coat assembly. Nat Rev Mol Cell Biol. 2006; 7(10):727–738. [PubMed: 16990852]
13. Kuge O, Dascher C, Orci L, Rowe T, Amherdt M, Plutner H, Ravazzola M, Tanigawa G, Rothman JE, Balch WE. Sar1 promotes vesicle budding from the endoplasmic reticulum but not Golgi compartments. J Cell Biol. 1994; 125(1):51–65. [PubMed: 8138575]
14. Mikosch M, Kaberich K, Homann U. ER export of KAT1 is correlated to the number of acidic residues within a triacidic motif. Traffic. 2009; 10(10):1481–1487. [PubMed: 19659502]
15. Wang X, Matteson J, An Y, Moyer B, Yoo JS, Bannykh S, Wilson IA, Riordan JR, Balch WE. COPII-dependent export of cystic fibrosis transmembrane conductance regulator from the ER uses a di-acidic exit code. J Cell Biol. 2004; 167(1):65–74. [PubMed: 15479737]
16. Nishimura N, Balch WE. A di-acidic signal required for selective export from the endoplasmic reticulum. Science. 1997; 277(5325):556–558. [PubMed: 9228004]
17. Nishimura N, Bannykh S, Slabough S, Matteson J, Altschuler Y, Hahn K, Balch WE. A di-acidic (DXE) code directs concentration of cargo during export from the endoplasmic reticulum. J Biol Chem. 1999; 274(22):15937–15946. [PubMed: 10336500]
18. Ma D, Zerangue N, Lin YF, Collins A, Yu M, Jan YN, Jan LY. Role of ER export signals in controlling surface potassium channel numbers. Science. 2001; 291(5502):316–319. [PubMed: 11209084]
19. Votsmeier C, Gallwitz D. An acidic sequence of a putative yeast Golgi membrane protein binds COPII and facilitates ER export. EMBO J. 2001; 20(23):6742–6750. [PubMed: 11726510]
20. Zuzarte M, Rinne S, Schlichthorl G, Schubert A, Daut J, Preisig-Muller R. A di-acidic sequence motif enhances the surface expression of the potassium channel TASK-3. Traffic. 2007; 8(8): 1093–1100. [PubMed: 17547699]
21. Sevier CS, Weisz OA, Davis M, Machamer CE. Efficient export of the vesicular stomatitis virus G protein from the endoplasmic reticulum requires a signal in the cytoplasmic tail that includes both tyrosine-based and di-acidic motifs. Mol Biol Cell. 2000; 11(1):13–22. [PubMed: 10637287]
22. Otte S, Barlowe C. The Erv41p-Erv46p complex: multiple export signals are required in trans for COPII-dependent transport from the ER. EMBO J. 2002; 21(22):6095–6104. [PubMed: 12426381]
23. Nufer O, Kappeler F, Guldbrandsen S, Hauri HP. ER export of ERGIC-53 is controlled by cooperation of targeting determinants in all three of its domains. J Cell Sci. 2003; 116(Pt 21): 4429–4440. [PubMed: 13130098]
24. Dominguez M, Dejgaard K, Fullekrug J, Dahan S, Fazel A, Paccaud JP, Thomas DY, Bergeron JJ, Nilsson T. gp25L/emp24/p24 protein family members of the cis-Golgi network bind both COP I and II coatomer. J Cell Biol. 1998; 140(4):751–765. [PubMed: 9472029]
25. Fiedler K, Veit M, Stamnes MA, Rothman JE. Bimodal interaction of coatomer with the p24 family of putative cargo receptors. Science. 1996; 273(5280):1396–1399. [PubMed: 8703076]
26. Farhan H, Reiterer V, Korkhov VM, Schmid JA, Freissmuth M, Sitte HH. Concentrative export from the endoplasmic reticulum of the gamma-aminobutyric acid transporter 1 requires binding to SEC24D. J Biol Chem. 2007; 282(10):7679–7689. [PubMed: 17210573]
27. Miller EA, Beilharz TH, Malkus PN, Lee MC, Hamamoto S, Orci L, Schekman R. Multiple cargo binding sites on the COPII subunit Sec24p ensure capture of diverse membrane proteins into transport vesicles. Cell. 2003; 114(4):497–509. [PubMed: 12941277]
28. Mancias JD, Goldberg J. Structural basis of cargo membrane protein discrimination by the human COPII coat machinery. EMBO J. 2008; 27(21):2918–2928. [PubMed: 18843296]
29. Mossessova E, Bickford LC, Goldberg J. SNARE selectivity of the COPII coat. Cell. 2003; 114(4): 483–495. [PubMed: 12941276]
30. Duvernay MT, Zhou F, Wu G. A conserved motif for the transport of G protein-coupled receptors from the endoplasmic reticulum to the cell surface. J Biol Chem. 2004; 279(29):30741–30750. [PubMed: 15123661]
31. Duvernay MT, Dong C, Zhang X, Zhou F, Nichols CD, Wu G. Anterograde trafficking of G protein-coupled receptors: function of the C-terminal F(X)6LL motif in export from the endoplasmic reticulum. Mol Pharmacol. 2009; 75(4):751–761. [PubMed: 19118123]
32. Bermak JC, Li M, Bullock C, Zhou QY. Regulation of transport of the dopamine D1 receptor by a new membrane-associated ER protein. Nat Cell Biol. 2001; 3(5):492–498. [PubMed: 11331877]

NIH-PA Author Manuscript

NIH-PA Author Manuscript

NIH-PA Author Manuscript

33. Dong C, Filipeanu CM, Duvernay MT, Wu G. Regulation of G protein-coupled receptor export trafficking. Biochim Biophys Acta. 2007; 1768(4):853–870. [PubMed: 17074298]
34. Robert J, Clauser E, Petit PX, Ventura MA. A novel C-terminal motif is necessary for the export of the vasopressin V1b/V3 receptor to the plasma membrane. J Biol Chem. 2005; 280(3):2300–2308. [PubMed: 15528211]
35. Donnellan PD, Kimbembe CC, Reid HM, Kinsella BT. Identification of a novel endoplasmic reticulum export motif within the eighth alpha-helical domain (alpha-H8) of the human prostacyclin receptor. Biochim Biophys Acta. 2011; 1808(4):1202–1218. [PubMed: 21223948]
36. Duvernay MT, Dong C, Zhang X, Robitaille M, Hebert TE, Wu G. A single conserved leucine residue on the first intracellular loop regulates ER export of G protein-coupled receptors. Traffic. 2009; 10(5):552–566. [PubMed: 19220814]
37. Margeta-Mitrovic M, Jan YN, Jan LY. A trafficking checkpoint controls GABA(B) receptor heterodimerization. Neuron. 2000; 27(1):97–106. [PubMed: 10939334]
38. Dong C, Wu G. Regulation of anterograde transport of alpha2-adrenergic receptors by the N termini at multiple intracellular compartments. J Biol Chem. 2006; 281(50):38543–38554. [PubMed: 17038316]
39. Kim J, Kleizen B, Choy R, Thinakaran G, Sisodia SS, Schekman RW. Biogenesis of gamma-secretase early in the secretory pathway. J Cell Biol. 2007; 179(5):951–963. [PubMed: 18056412]
40. Miller E, Antonny B, Hamamoto S, Schekman R. Cargo selection into COPII vesicles is driven by the Sec24p subunit. EMBO J. 2002; 21(22):6105–6113. [PubMed: 12426382]
41. Wendeler MW, Paccaud JP, Hauri HP. Role of Sec24 isoforms in selective export of membrane proteins from the endoplasmic reticulum. EMBO Rep. 2007; 8(3):258–264. [PubMed: 17255961]
42. Jackson MR, Nilsson T, Peterson PA. Identification of a consensus motif for retention of transmembrane proteins in the endoplasmic reticulum. EMBO J. 1990; 9(10):3153–3162. [PubMed: 2120038]
43. Giraudo CG, Maccioni HJ. Endoplasmic reticulum export of glycosyltransferases depends on interaction of a cytoplasmic dibasic motif with Sar1. Mol Biol Cell. 2003; 14(9):3753–3766. [PubMed: 12972562]
44. Pao CS, Benovic JL. Structure/function analysis of alpha2A-adrenergic receptor interaction with G protein-coupled receptor kinase 2. J Biol Chem. 2005; 280(12):11052–11058. [PubMed: 15653687]
45. DeGraff JL, Gurevich VV, Benovic JL. The third intracellular loop of alpha 2-adrenergic receptors determines subtype specificity of arrestin interaction. J Biol Chem. 2002; 277(45):43247–43252. [PubMed: 12205092]
46. Wang Q, Limbird LE. Regulated interactions of the alpha 2A adrenergic receptor with spinophilin, 14-3-3zeta, and arrestin 3. J Biol Chem. 2002; 277(52):50589–50596. [PubMed: 12376539]
47. Wu G, Zhao G, He Y. Distinct pathways for the trafficking of angiotensin II and adrenergic receptors from the endoplasmic reticulum to the cell surface: Rab1-independent transport of a G protein-coupled receptor. J Biol Chem. 2003; 278(47):47062–47069. [PubMed: 12970354]
48. Kallal L, Gagnon AW, Penn RB, Benovic JL. Visualization of agonist-induced sequestration and down-regulation of a green fluorescent protein-tagged beta2-adrenergic receptor. J Biol Chem. 1998; 273(1):322–328. [PubMed: 9417083]
49. Hunyady L, Baukal AJ, Gaborik Z, Olivares-Reyes JA, Bor M, Szaszak M, Lodge R, Catt KJ, Balla T. Differential PI 3-kinase dependence of early and late phases of recycling of the internalized AT1 angiotensin receptor. J Cell Biol. 2002; 157(7):1211–1222. [PubMed: 12070129]
50. Dong C, Yang L, Zhang X, Gu H, Lam ML, Claycomb WC, Xia H, Wu G. Rab8 interacts with distinct motifs in {alpha}2B- and {beta}2-adrenergic receptors and differentially modulates their transport. J Biol Chem. 2010; 285(26):20369–20380. [PubMed: 20424170]
51. Dong C, Li C, Wu G. Regulation of alpha2B-Adrenergic Receptor-mediated Extracellular Signal-regulated Kinase 1/2 (ERK1/2) Activation by ADP-ribosylation Factor 1. J Biol Chem. 2011; 286(50):43361–43369. [PubMed: 22025613]

NIH-PA Author Manuscript

NIH-PA Author Manuscript

NIH-PA Author Manuscript

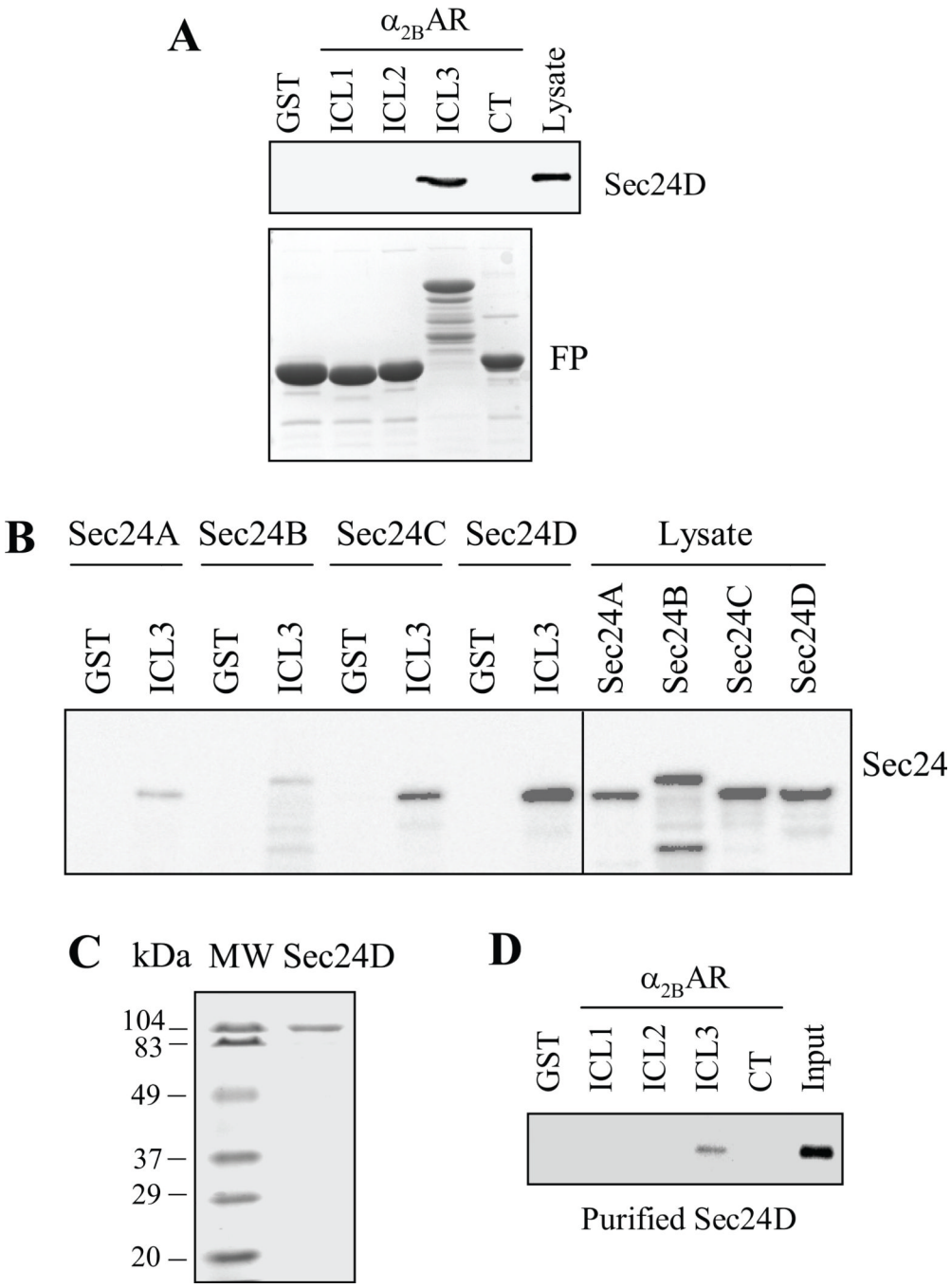

Fig. 1. Interaction of the third intracellular loop of α_{2B}-AR with Sec24

(A) Interaction of intracellular domains of α_{2B}-AR with Sec24D. The first (ICL1), the second (ICL2) and the third (ICL3) intracellular loops and the C-terminus (CT) of α_{2B}-AR were generated as GST fusion proteins (FP, bottom panel). Sec24D tagged with GFP was expressed in HEK293 cells and total cell homogenates were incubated with the purified GST fusion proteins as described in "Experimental procedures". Sec24D bound to the GST fusion proteins was revealed by immunoblotting using anti-GFP antibodies (upper panel). (B) ICL3 interaction with Sec24A, Sec24B, Sec24C, and Sec24D isoforms. Each Sec24 isoform tagged with GFP was transiently expressed in HEK293 cells and their interaction with the ICL3 was determined by the GST pull-down assay. (C) Sec24D (1 μg) purified from insect

Sf9 cells, separated by SDS-PAGE, and stained with Coomassie Brilliant Blue R250. MW – molecular weight standards. (D) The interaction of intracellular domains of α_{2B}-AR with purified Sec24D. In each panel, similar results were obtained in at least three separate experiments.

NIH-PA Author Manuscript
NIH-PA Author Manuscript
NIH-PA Author Manuscript

NIH-PA Author Manuscript

NIH-PA Author Manuscript

NIH-PA Author Manuscript

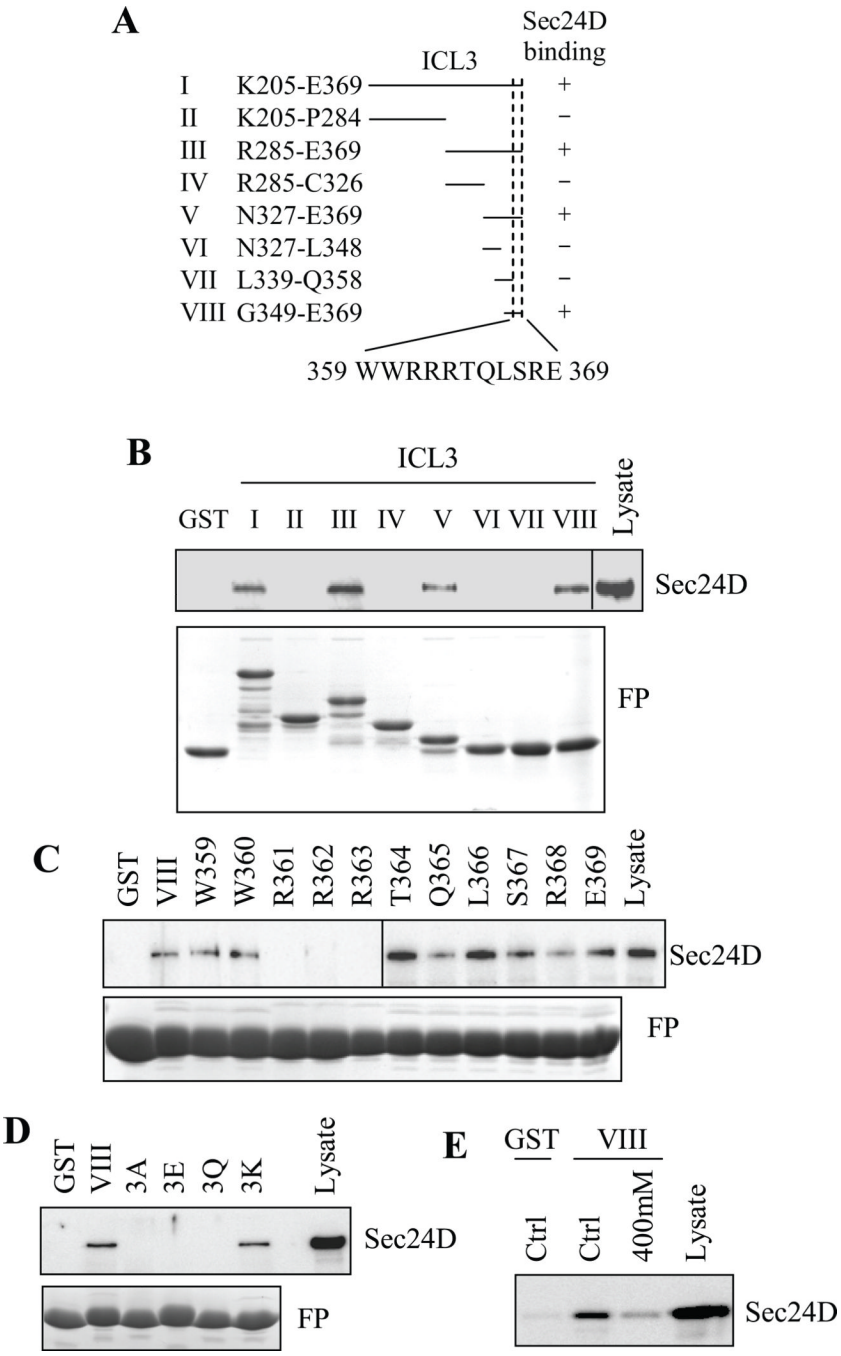

Fig. 2. Identification of the Sec24-binding site in α_{2B}-AR

(A) A summary of progressive deletion to identify the Sec24D-binding domain in the ICL3 of α_{2B}-AR. +, interacting with Sec24D; −, not interacting with Sec24D. This strategy identifies the Sec24D-binding site in the region from W359 to E369. (B) A representative blot showing the interaction of different ICL3 fragments with Sec24D. Each fragment of the ICL3 was generated as GST fusion proteins (FP, lower panel) and their interaction with GFP-tagged Sec24D determined (upper panel). (C) Site-directed alanine scanning mutagenesis to identify the Sec24D-binding site in α_{2B}-AR. The ICL3 fragment G349-E369 (VIII) and its mutants in which each residue in the Sec24-binding domain W359-E369 as identified in Fig. 2A was individually mutated to Ala were generated as GST fusion proteins

NIH-PA Author Manuscript

NIH-PA Author Manuscript

NIH-PA Author Manuscript

(lower panel) and their abilities to interact with Sec24D were determined (upper panel). (D) Effect of the combinational mutation of three Arg residues at positions 361, 362 and 363 (3R) to three Ala (3A), three Glu (3E), three Gln (3Q) and three Lys (3K) on the ICL3 interaction with Sec24D. The ICL3 fragment G349-E369 (VIII) and its mutants were generated as GST fusion proteins (lower panel) and their interaction with Sec24D were determined (upper panel). (E) Effect of NaCl on the ICL3 interaction with Sec24D. The ICL3 fragment G349-E369 (VIII) generated as GST fusion protein was incubated with Sec24D in the binding buffer containing 120 mM (Ctrl) or 400 mM NaCl. In panels (B) through (E) similar results were obtained in at least four different experiments.

NIH-PA Author Manuscript

NIH-PA Author Manuscript

NIH-PA Author Manuscript

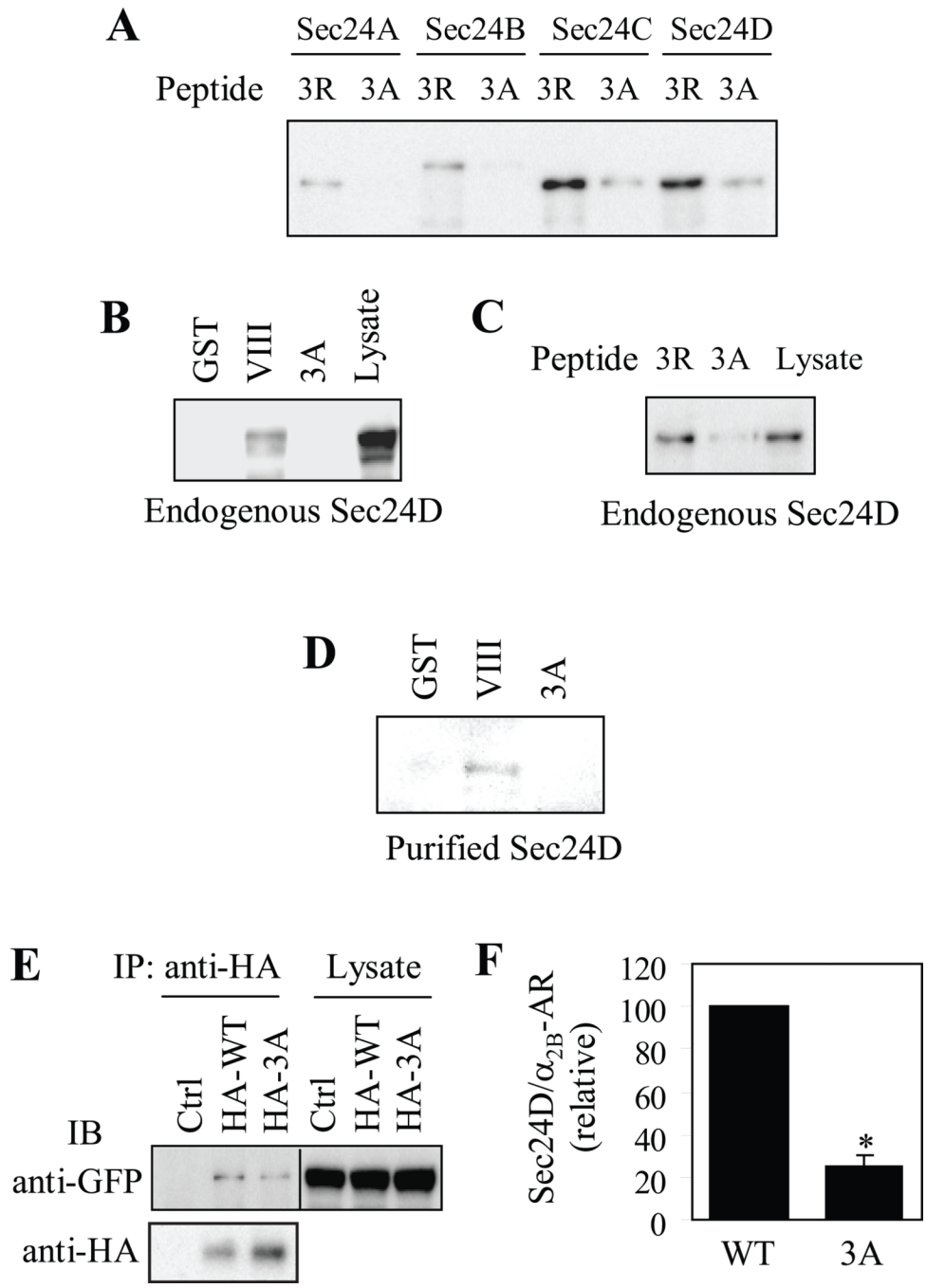

Fig. 3. The 3R motif-dependent interaction of α_{2B}-AR with Sec24

(A) Interaction of the ICL3-conjugated agarose beads with Sec24A, Sec24B, Sec24C and Sec24D. The ICL3 fragment G349-E369 containing the 3R motif (3R) or its mutant in which the 3R motif was mutated to three alanines (3A) were synthesized and conjugated to agarose. Each Sec24 isoform tagged with GFP was transiently expressed in HEK293 cells and total cell homogenates were incubated with the ICL3-conjugated agarose beads. Bound Sec24 was revealed by immunoblotting using anti-GFP antibodies. (B) The ICL3 interaction with endogenous Sec24D. The ICL3 fragment G349-E369 (VIII) and its 3A mutant were generated as GST fusion proteins and incubated with total homogenates prepared from HEK293 cells. Bound Sec24D was determined by immunoblotting using anti-Sec24D

NIH-PA Author Manuscript

NIH-PA Author Manuscript

NIH-PA Author Manuscript

antibodies. (C) Interaction of the ICL3-conjugated agarose beads with endogenous Sec24D. (D) Effect of mutating the 3R motif on the interaction of the ICL3 with Sec24D purified from insect Sf9 cells. In panels A through D, similar results were obtained in at least three independent experiments. (E) Interaction of full-length α_{2B}-AR with Sec24D by co-immunoprecipitation. HEK293 cells were transiently transfected with pcDNA3.1 empty vector (Ctrl), HA-tagged α_{2B}-AR (HA-WT) or HA-tagged α_{2B}-AR mutant in which the 3R motif was mutated to 3A (HA-3A) together with GFP-tagged Sec24D. The cells were solubilized and the receptors were immunoprecipitated with anti-HA antibodies. The immunoprecipitate was separated by SDS-PAGE and the level of Sec24D in the HA-immunoprecipitate was determined by immunoblotting using anti-GFP antibodies (upper panel) and the immunoprecipitated receptor revealed using anti-HA antibodies (lower panel). (F) Quantitative data of interaction between α_{2B}-AR and Sec24D by co-immunoprecipitation. The data shown are the percentage of the mean value obtained from cells expressing α_{2B}-AR and are presented as the mean ± S.E. of three experiments.*, $P < 0.05$ versus WT.

NIH-PA Author Manuscript
NIH-PA Author Manuscript
NIH-PA Author Manuscript

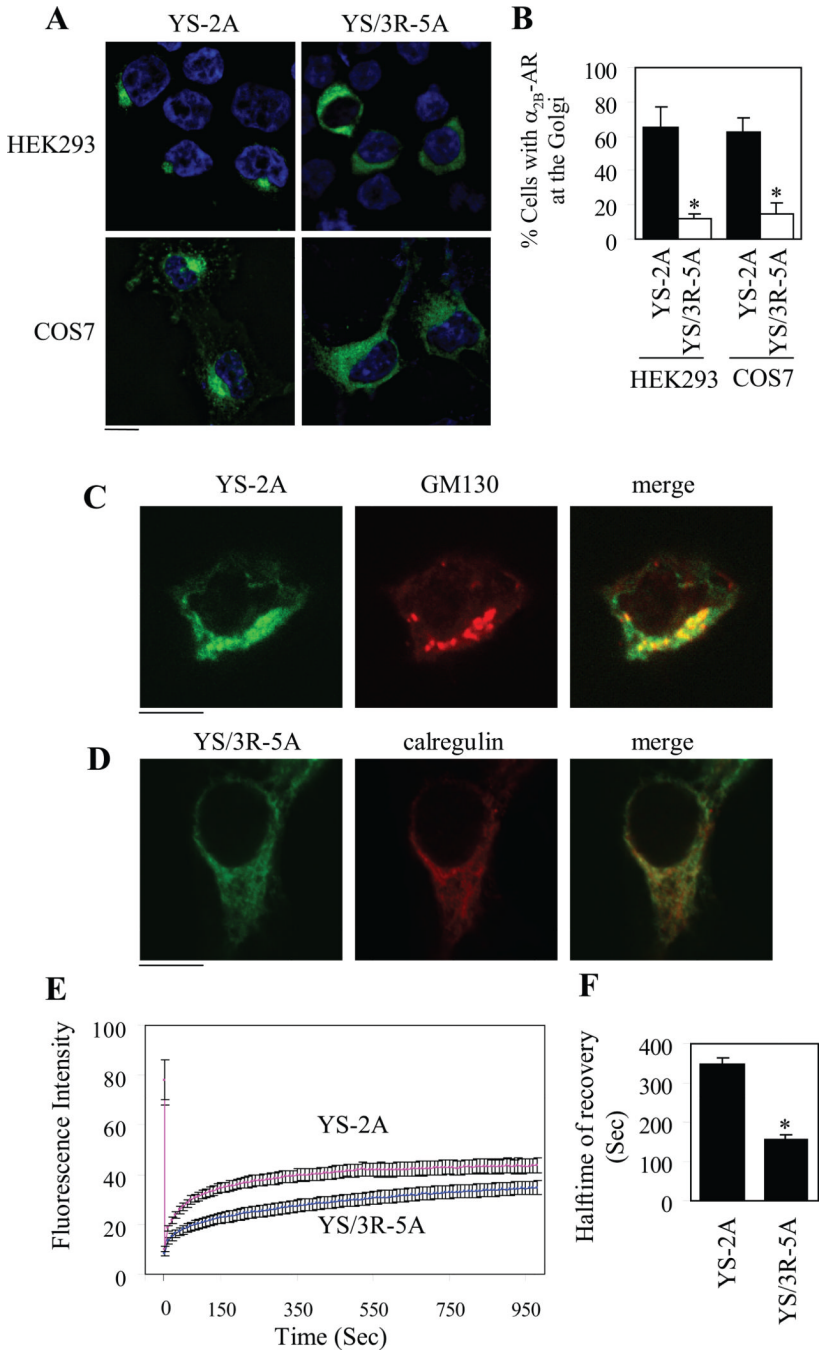

Fig. 4. Effect of mutating the 3R motif on the export of α_{2B}-AR from the ER

(A) Subcellular distribution of the YS-2A mutant in which the N-terminal YS motif were mutated to Ala and the YS/3R-5A mutant in which both the YS and 3R motifs were mutated to Ala. The α_{2B}-AR mutants were tagged with GFP and transiently expressed in HEK293 cells. Their subcellular distribution was visualized by fluorescence microscopy. (B) Quantitative data shown in A. Approximately 100 cells were counted in each experiment. Data are means ± SE (n = 3). (C) Co-localization of the α_{2B}-AR mutant YS-2A with the Golgi marker GM130. (D) Co-localization of the α_{2B}-AR mutant YS/3R-5A with the ER marker calregulin. HEK293 cells were transfected with the α_{2B}-AR mutant and its co-localization with the Golgi or ER markers were revealed by fluorescence microscopy

following staining with antibodies against GM130 (C) and calregulin (D). *Green*, α_{2B}-AR mutant tagged with GFP; *red*, GM130 (C) or calregulin (D); *yellow*, co-localization of the mutated receptors with the Golgi (C) and the ER (D) markers. The data shown in (C) and (D) are representative images of at least three independent experiments. (E) Recovery curves of the Golgi fluorescence in COS7 cells expressing the GFP-tagged YS-2A and YS/3R-5A mutants after photobleaching. (F) Half-times of the recovery of the Golgi-localized YS-2A and YS/3R-5A mutants. The data are presented as the mean ± S.E. of 20 cells in 6 separate experiments.*, $P < 0.05$ versus YS-2A. Scale bar, 10 μm.

NIH-PA Author Manuscript
NIH-PA Author Manuscript
NIH-PA Author Manuscript

NIH-PA Author Manuscript

NIH-PA Author Manuscript

NIH-PA Author Manuscript

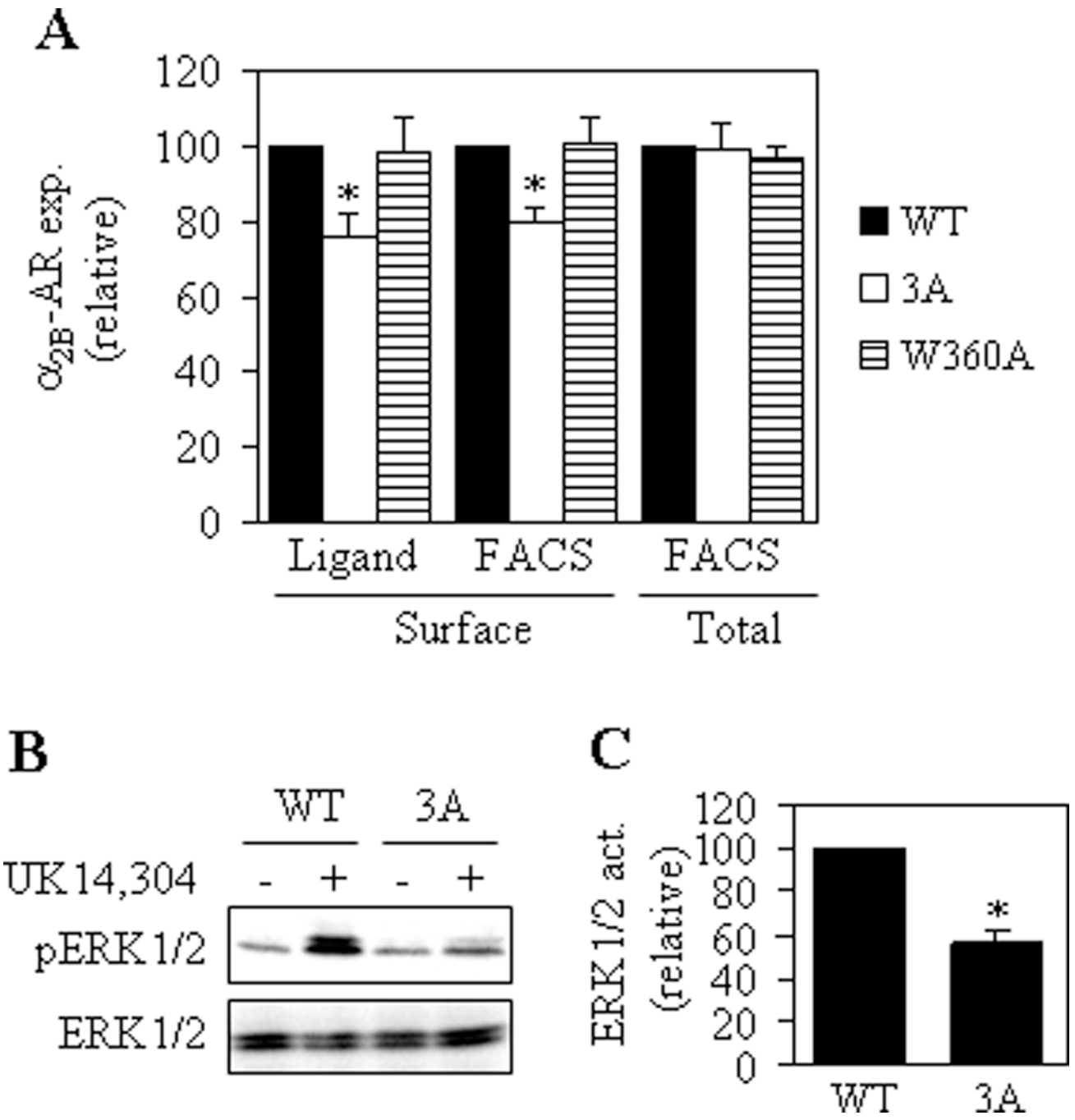

Fig. 5. Effect of mutating the 3R motif on the cell surface expression and signaling of α_{2B}-AR

(A) Effect of mutating the 3R motif on the cell surface and total expression of α_{2B}-AR. HEK293 cells cultured on 6-well plates were transfected with HA- or GFP-tagged α_{2B}-AR (WT) or its 3A and W360A mutants. The cell surface expression of α_{2B}-AR was determined either by intact cell ligand binding using [^{3}H]-RX821002 or by FACS following staining with anti-HA antibodies in non-permeabilized cells and the total expression was measured by FACS detecting the GFP signal. The data shown are the percentages of the mean value obtained from cells transfected with wild-type α_{2B}-AR and are presented as the mean ± S.E. of at least five separate experiments. (B) Effect of mutating the 3R motif on α_{2B}-AR-mediated ERK1/2 activation. HEK293 cells were transfected with α_{2B}-AR or its 3A mutant

NIH-PA Author Manuscript

NIH-PA Author Manuscript

NIH-PA Author Manuscript

and stimulated with UK14,304 at a concentration of 1 μM for 5 min at 37 °C. ERK1/2 activation was determined by immunoblotting using phospho-specific ERK1/2 antibodies and total ERK1/2 expression determined by anti-ERK1/2 antibodies. (C) Qantitative data showing the effect of mutating the 3R motif on α_{2B}-AR-mediated ERK1/2 activation. The data shown are the percentages of the mean value obtained from cells transfected with WT α_{2B}-AR and are presented as the mean ± S.E. of three experiments.*, $P < 0.05$ versus WT.

NIH-PA Author Manuscript

NIH-PA Author Manuscript

NIH-PA Author Manuscript

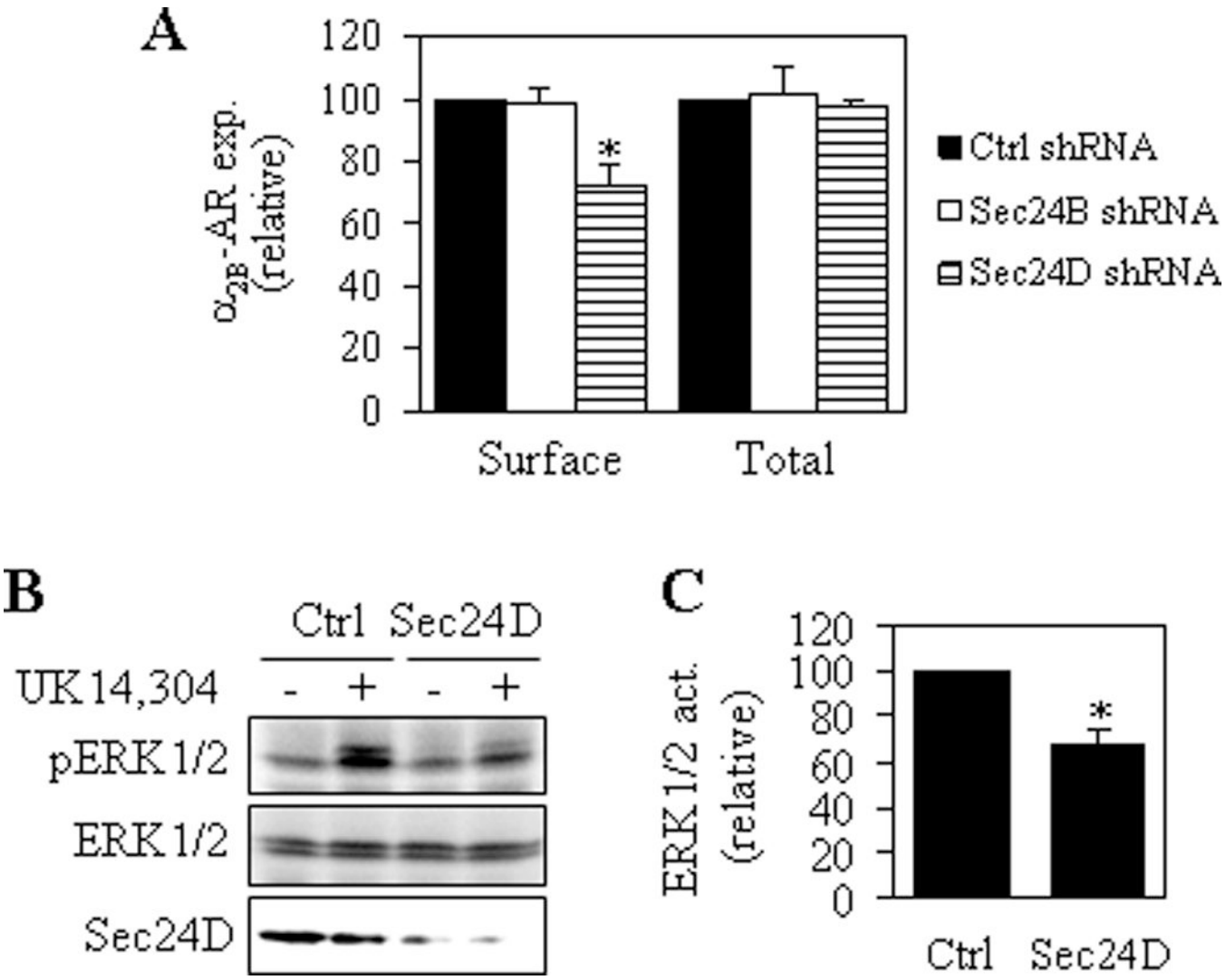

Fig. 6. Effect of shRNA-mediated knockdown of Sec24 on the cell surface expression and signaling of α_{2B}-AR

(A) Effect of shRNA-mediated knockdown of Sec24 on the cell surface expression of α_{2B}-AR. HEK293 cells cultured on 6-well plates were cotransfected with α_{2B}-AR together with control or Sec24 shRNA. The cell surface expression of α_{2B}-AR was determined by intact cell ligand binding using [^{3}H]-RX821002. The total receptor expression was measured by FACS detecting the GFP signal. (B) Effect of shRNA-mediated Sec24D knockdown on α_{2B}-AR-mediated ERK1/2 activation. HEK293 cells were transfected with α_{2B}-AR together with control shRNA or Sec24D shRNA. ERK1/2 activation in response to UK14304 stimulation was determined. (C) Quantitative data showing the effect of shRNA-mediated Sec24D knockdown on α_{2B}-AR-mediated ERK1/2 activation. The data shown are the percentages of the mean value obtained from cells transfected with control shRNA vector and are presented as the mean ± S.E. of three experiments.*, $P < 0.05$ versus Ctrl.

NIH-PA Author Manuscript

NIH-PA Author Manuscript

NIH-PA Author Manuscript

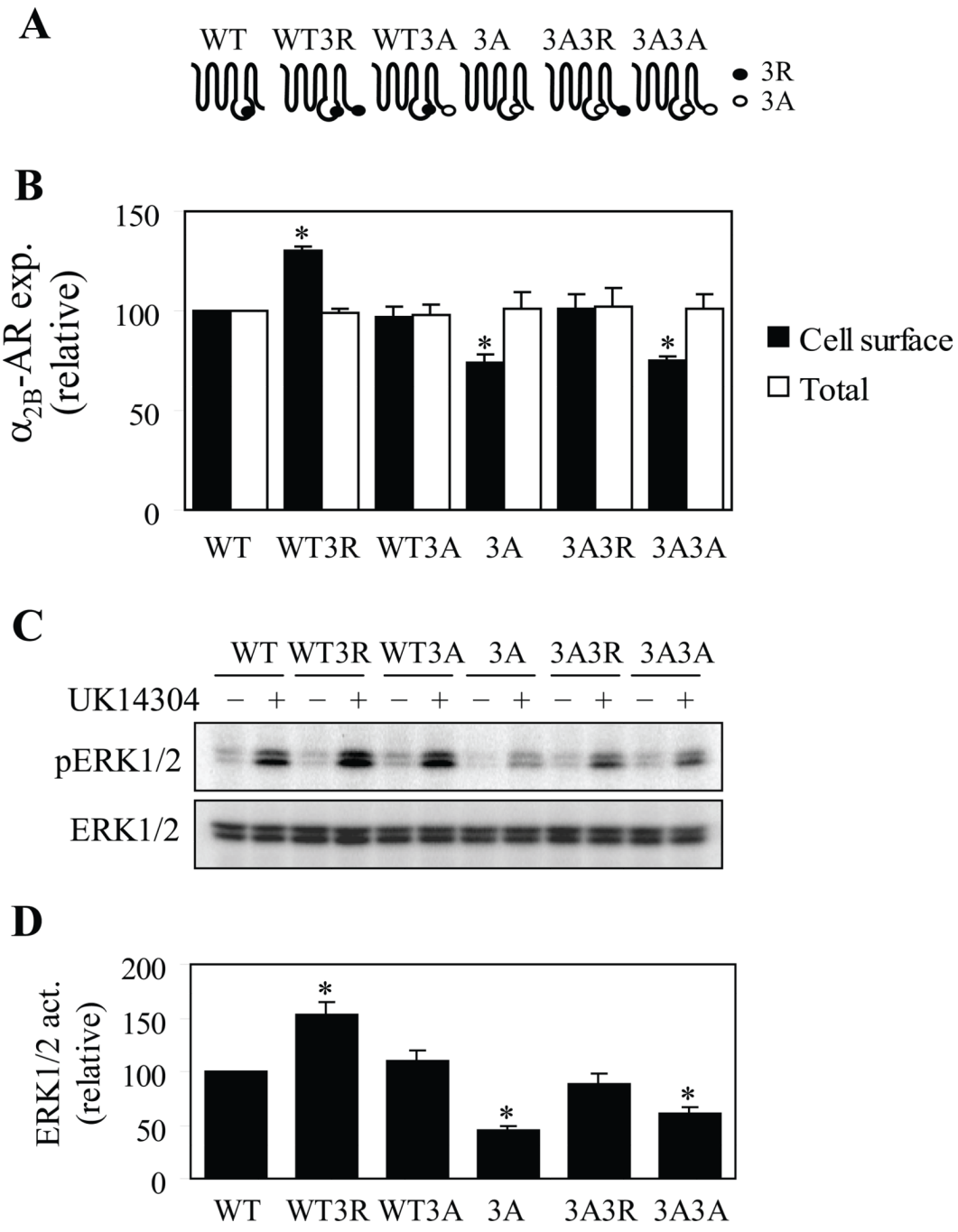

Fig. 7. Effect of the 3R motif when transferred to the C-terminus on the cell surface expression and signaling of α_{2B}-AR

(A) A diagram showing generation of different α_{2B}-AR mutants, in which the 3R motif was added to the C-terminus of α_{2B}-AR (WT3R), the 3A motif was added to the C-terminus of α_{2B}-AR (WT3A), the 3R motif were mutated to 3A (3A), the 3R motif was added to the C-terminus of the 3A mutant (3A3R) or the 3A motif was added to the C-terminus of the 3A mutant (3A3A). (B) The cell surface expression of α_{2B}-AR and its various mutants. α_{2B}-AR and its mutants were transiently expressed in HEK293 cells. Their cell surface was measured by intact cell ligand binding using [^{3}H]-RX821002 and the total expression by FACS. The data shown are the percentages of the mean value obtained from cells

transfected with wild-type α_{2B}-AR and are presented as the mean ± S.E. of six experiments. (C) ERK1/2 activation by α_{2B}-AR and its mutants. HEK293 cells were transiently transfected with α_{2B}-AR or its mutants and ERK1/2 activation in response to UK14304 stimulation was measured. (D) Quantitative data of ERK1/2 activation by α_{2B}-AR and its mutants. The data shown are the percentages of ERK1/2 activation obtained from cells transfected with wild-type α_{2B}-AR (WT) and presented as the mean ± S.E. of three independent experiments. * and ** < 0.05 versus WT; **, P < 0.05 versus 3AR.

NIH-PA Author Manuscript
NIH-PA Author Manuscript
NIH-PA Author Manuscript

NIH-PA Author Manuscript

NIH-PA Author Manuscript

NIH-PA Author Manuscript

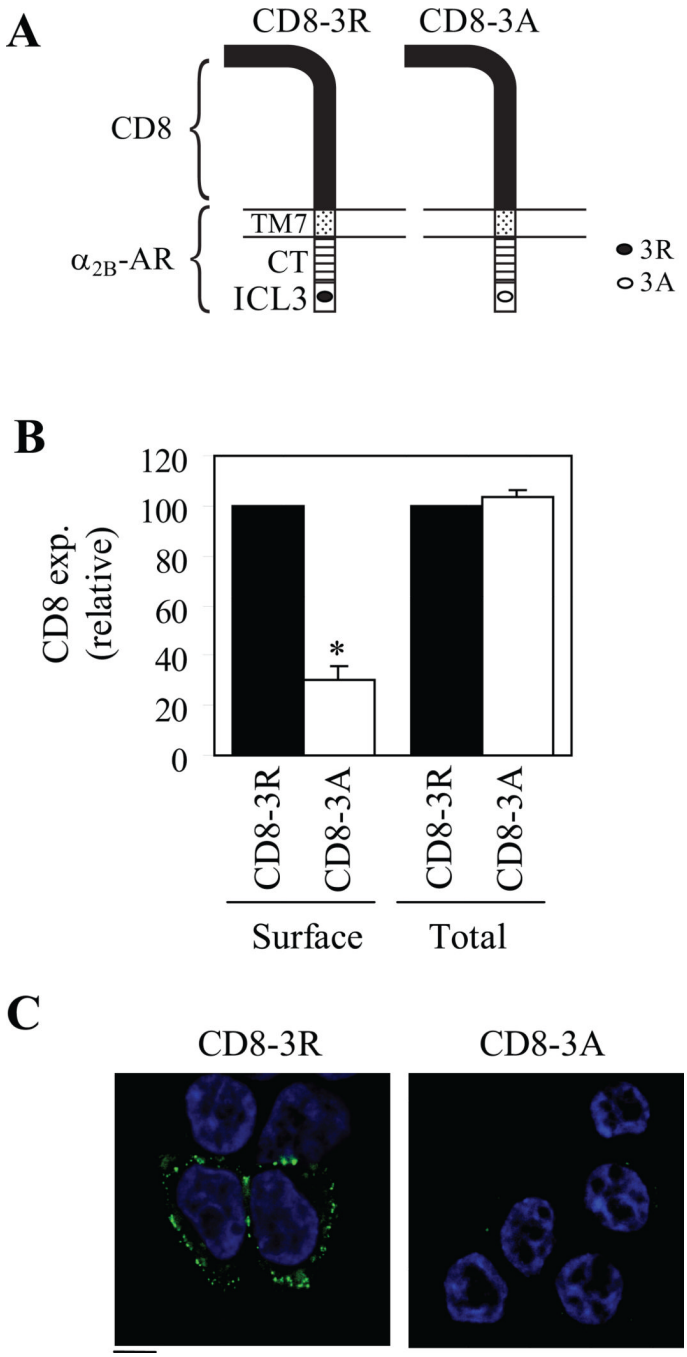

Fig. 8. Effect of the 3R motif of α_{2B}-AR on the cell surface export of CD8 glycoprotein

(A) A diagram showing generation of chimeric α_{2B}-AR-CD8 proteins. The truncated α_{2B}-AR containing the 7th transmembrane (TM7) and the C-terminus (CT) of α_{2B}-AR was conjugated with the N-terminal portion of CD8 glycoprotein and an ICL3 fragment containing the 3R motif (CD8-3R) or the 3A motif (CD8-3A) at the C-terminus. (B) Cell surface expression of CD8-3R and CD8-3A. CD8-3R and CD8-3A were transiently expressed in HEK293 cells and their cell surface expression was measured by FACS following staining using anti-CD8 antibodies in nonpermeabilized cells. The total expression of the chimeric proteins was measured by FACS after staining with anti-CD8 antibodies in permeabilized cells. The data shown are the percentages of the mean value obtained from

cells transfected with CD8-3R and are presented as the mean ± S.E. of four experiments. (C) HEK293 cells were transfected with CD8-3R or CD8-3A and their cell surface was visualized by fluorescence microscopy following staining using anti-CD8 antibodies in nonpermeabilized cells.

NIH-PA Author Manuscript
NIH-PA Author Manuscript
NIH-PA Author Manuscript

NIH-PA Author Manuscript

NIH-PA Author Manuscript

NIH-PA Author Manuscript

α_{2B}-AR	AIGGQWW**RRR**AQLTREKRFTFV
α_{2C}-AR	RARSSVC**RRK**VAQAREKR
β_1-AR	LANGRAG**KRR**PSRLVALREQKA
M1-MR	RGKEQLA**KRK**TFSLVKEKKAAR
M2-MR	KMTKQPA**KKK**PPPSREKKVTRT
M3-MR	TRSQIT**KRKR**MSLVKEKKAAQT
M5-MR	PSHQMT**KRKR**VVLVKERKAAQT
D2	TSLKTMS**RRK**LSQQKEKKATQ
D4	TPPQT**RRRRR**AKITGRERKAMR
5HT1A	NERNAEA**KRK**MALARERKTVK
5HT1B	VSDALLE**KKK**LMAARERKATKT
5HT1D	LADSALE**RKR**ISAARERKATKI
5HT2C	**RRRKKK**ERRPRGTMQAIN
BRS3	ARKQIES**RKR**IART
NMB-R	TKKQMET**RKR**LAK
GPRP	VKKQIES**RKR**LAK
APJ	RIEGL**RKRRR**
PRLHR	ADWDRA**RRRR**T
NTR2	GGQVSLV**RHK**DVRRIRSLQRSV
SSR1	LKAGWQQ**RKR**SERKIT
SSR2	IRVGSS**KRKK**SEKK
SSR3	WAPSCQ**RRRR**SERRVTR
SSR4	LRAGWQQ**RRR**SEKKITRL
SSR5	WAPSCQ**RRRR**SERRVT
NK1R	YHEQVSA**KRK**VVK
NK2R	NLRHLQA**KKK**FVKT
NK3R	YHEQLKA**KRK**VVKM
GALR1	SKKSEAS**KKK**TAQT
GALR2	GSGARRA**KRK**VTRM
GLAR3	GAAAAEA**RRR**ATGRAGRA
PAR2	DENSE**KKRKR**A
GP182	QPGQPKS**RRH**CL
RL3R2	LQRRQ**RRR**QDSRVVARSVR
PKR1	GFQTEQI**RKR**LRC**RRK**T
PYR2	GFQTEQI**RKR**LRC**RRK**T
PE2R4	PRLSDF**RRRR**SFRRIAGAE
PE2R1	ALLRARW**RRR**SRRPPPA..**RRR**
PE2R2	LIRM**HRR**SRRSRCG..**RRR**
PD2R	MRNLYAM**HRR**LQRHPRSCTRDC
PI2R	CRMYRQQ**KRH**QGSLGPRPRTGE
P2RY1	DLDNSPL**RRK**SIYLVIIV
P2RY2	SGGLPRA**KRK**SVRT
P2RY9	LSQIGTN**KKK**VLKMITVH
P2Y12	RGVGKVP**RKK**
P2Y14	SRNSTSV**KKK**SSRN
P2RY8	EAHGREQ**RRR**AVG
GPR92	DATQSQ**RRRK**TVRLLLAN
GPR87	FISQSS**RKRK**HNQSIRV
PTAFR	QQRNAEV**KRR**ALWM
MTR1B	WVLVLQA**RRK**AKPESRLCLKPS
EDG4	RIFFYV**RRR**VQMAEHVSCHPR
EDG6	KAPRPAA**RRK**ARRLLKT
EDG7	RIYVYV**KRK**TNVLSPH..**RRR**
EDG8	GTTSTRA**RRK**PRSLALLRT
V2R	PSERPGG**RRR**GRRTGSPGEGAH

Fig. 9. The conserved basic residue clusters in the third intracellular loops of GPCRs

The data were constructed from the alignments described in the GPCRDB (www.gpcr.org). Human sequences are shown when available. AR, adrenergic receptor; MR, muscarinic receptor; D, dopamine receptor; HT, ydroxytryptamine receptor; BRS3, bombesin receptor subtype 3; NMB-R, neuromedin B receptor; GPRP, gastrin-releasing peptide receptor; APJ, apelin receptor; PRLHR, prolactin releasing hormone receptor; NTR2, eurotensin receptor type 2; SSR, somatostatin receptor; NKR, neurokinin receptor; GALR, galanin receptor; PAR, proteinase-activated receptor; GP182, G protein-coupled receptor 182; RL3R2, relaxin-3 receptor 2; PKR, prokineticin receptor; PE2R4, prostaglandin E2 receptor EP4 subtype; PD2R, prostaglandin D2 receptor; PI2R, prostaglandin I2 receptor; P2RY1,

purinergic receptor P2Y1; PTAFR, platelet-activating factor receptor; MTR, melatonin receptor; EDG, Edg receptor; V2R, vasopressin V2 receptor.

NIH-PA Author Manuscript

NIH-PA Author Manuscript

NIH-PA Author Manuscript